Information Sciences 441 (2018) 41–49

Contents lists available at ScienceDirect

Information Sciences

journal homepage: www.elsevier.com/locate/ins

Deep convolution neural network for accurate diagnosis of glaucoma using digital fundus images

U Raghavendra[a], Hamido Fujita[b,*], Sulatha V Bhandary[c], Anjan Gudigar[a], Jen Hong Tan[d], U Rajendra Acharya[d,e,f]

[a] Department of Instrumentation and Control Engineering, Manipal Institute of Technology, Manipal Academy of Higher Education, Manipal 576104, India
[b] Faculty of Software and Information Science, Iwate Prefectural University (IPU), Iwate 020-0693, Japan
[c] Department of Ophthalmology, Kasturba Medical College, Manipal Academy of Higher Education, Manipal 576104, India
[d] Department of Electronics and Computer Engineering, Ngee Ann Polytechnic, Singapore 599489, Singapore
[e] Department of Biomedical Engineering, School of Science and Technology, SUSS University, Singapore 599491, Singapore
[f] Department of Biomedical Engineering, Faculty of Engineering, University of Malaya, Kuala Lumpur, Malaysia

ARTICLE INFO

Article history:
Received 23 November 2017
Revised 23 December 2017
Accepted 31 January 2018
Available online 2 February 2018

Keywords:
CAD
CNN
Deep learning technique
Glaucoma

ABSTRACT

Glaucoma progressively affects the optic nerve and may cause partial or complete vision loss. Raised intravascular pressure is the only factor which can be modified to prevent blindness from this condition. Accurate early detection and continuous screening may prevent the vision loss. Computer aided diagnosis (CAD) is a non-invasive technique which can detect the glaucoma in its early stage using digital fundus images. Developing such a system require diverse huge database in order to reach optimum performance. This paper proposes a novel CAD tool for the accurate detection of glaucoma using deep learning technique. An *eighteen* layer convolutional neural networks (CNN) is effectively trained in order to extract robust features from the digital fundus images. Finally these features are classified into normal and glaucoma classes during testing. We have achieved the highest accuracy of 98.13% using 1426 (589: normal and 837: glaucoma) fundus images. Our experimental results demonstrates the robustness of the system, which can be used as a supplementary tool for the clinicians to validate their decisions.

1. Introduction

Glaucoma refers to the progressive loss of the retinal ganglion cells (RGC) leading to the visual loss. It results in varying degrees of irreversible visual disability and in some cases blindness. According to the World Health Organization (WHO), glaucoma is the second leading cause of blindness worldwide after cataracts [1,38]. The retinal nerve fibers are typically represented by the annular region between optic disc and the cup boundary, which is known as neuro retinal rim [2,36]. The fluid pressure in the inner portion of the eye is called intraocular pressure (IOP) [35,39]. Increase in this IOP leads to blockage of outflow of aqueous humor. This damages the optic nerve, which is essential to communicate the information from retina to the brain (Ref. Fig. 1) [37,38]. This deterioration of optic nerve fibers results in thickening of retinal nerve fiber layer (RNFL), which is usually known as 'cupping'. This cupping causes the progression of glaucoma [36,40]. The decrease

* Corresponding author.
E-mail address: HFujita-799@acm.org (H. Fujita).

https://doi.org/10.1016/j.ins.2018.01.051
0020-0255/

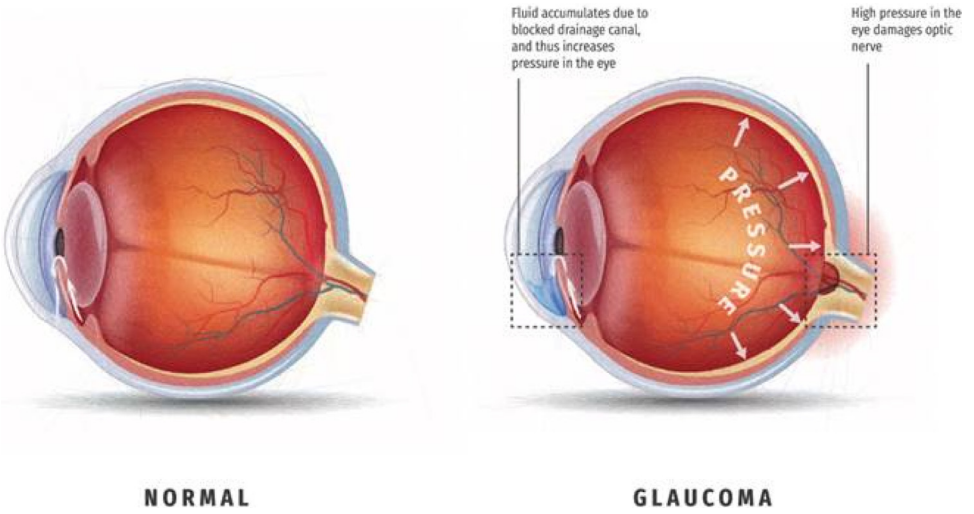

Fig. 1. Anatomy of normal and glaucoma eye.

in the healthy neuro retinal tissues can be easily noticed by measuring cup to disc ratio (CDR), which is an indication of glaucomatous change [40]. Typical value of CDR for a healthy eye is 0.3 [39,41].

1.1. Clinical diagnosis of Glaucoma

The clinical diagnosis of glaucoma includes a series of various tests that is carried out by the ophthalmologist. The key to prevent glaucoma is to have regular eye check-ups after 40 years. The following different tests are commonly performed to diagnose glaucoma are described as follows [3]:

Tonometry measures the pressure within the eye. During tonometry, eye drops are used to numb the eye. Then a doctor or technician uses a device called a tonometer to measure the inner pressure of the eye. If it exceeds >21 mm Hg, the person is diagnosed with glaucoma [4]. In *Ophthalmoscopy* the doctor examine the optic nerve for glaucoma damage. Eye drops are used to dilate the pupil so that the doctor can see through the eye to examine the shape and color of the optic nerve. If the intraocular pressure is not within the normal range or if the optic nerve looks unusual, the patient has to go through *Perimetry* which is a test to chart the visual field. High IOP in the eye can damage OD in glaucoma. *Gonioscopy* [4]. *Pachymetry* is a simple test, which measures cornea thickness. It helps in clinical diagnosis as it has great influence on eye pressure reading [4].

The clinical diagnosis of eye using above techniques is time consuming and involves inter/intra observer variability. Digital fundus images captured using a fundus camera can be effectively utilized for observing the progression of the diabetic retinopathy (DR), glaucoma and age related macular degeneration (AMD). The interesting clinical features of eye such as retina, optic disc, blood vessels etc., can be clearly visualized in fundus images. In addition, fundus camera is reliable, less expensive and easy to operate and it can be used to measure various structures such as change in cup to disc ratio, optic nerve head (ONH), cup diameter etc. [41]. Hence, fundus images can be effectively utilized as a cost effective tool for the diagnosis of retinal health [35,42] and eye abnormalities (DR, AMD and glaucoma) using a single fundus image.

Computer aided diagnosis (CAD) of fundus images helps to diagnose the retinal health using various computational algorithms. It is a cost effective tool which can avoid inter/intra observer variability which may be encountered in clinical diagnosis.

1.2. CAD for glaucoma

CAD has a major role in the diagnosis of glaucoma which can bring down the inter/intra observer variability. Also it requires minimum diagnosis time for more number of patients [5,6,18,34,35].

The detailed reviews of the existing work on CAD for glaucoma using digital fundus image are summarized in Table 1. It is observed that most of the algorithms follow the two stage pipeline structure: feature extraction and classification. The Wavelet Transform [9,10,14,15,22], Gabor transform [5], Higher order spectra (HOS) [8,12,23], etc., are the feature extraction techniques. In classification, artificial neural network (ANN) [2,14,21], support vector machine (SVM) [5,9,10], K-nearest neighbor (KNN) [13,19,24], etc., are used to predict the classes. The design of such hand-crafted features is tedious job and time consuming. These features are strongly related to expert knowledge and having restricted representation power. Thus, for a huge dataset it cannot show the discriminative power. To overcome this problem and enhance the classification performance, deep features are essential.

Table 1
State-of-the-art techniques proposed for the detection of glaucoma.

Author	Methods/features	Classifier	Number of images	Performance (%)
Nayak et al. [2]	Cup to disc ratio (CDR)	Artificial neural network	61	G_{sen}: 100 G_{spe}: 80
Noronha et al. [8]	HOS cumulants features	Naïve Bayesian	272	G_{acc}: 84.72 (two class) G_{acc}: 92.65 (three class) G_{sen}: 100 G_{spe}: 92
Acharya et al. [5]	Various features from Gabor transform	SVM	510	G_{acc}: 93.10 G_{sen}: 89.75 G_{spe}: 96.20
Mookiah et al. [9]	HOS and discrete wavelet transform based features	SVM	60	G_{acc}: 95 G_{sen}: 93.33 G_{spe}: 96.67
Maheshwari et al. [10]	Empirical wavelet transform and correntropy features	LS-SVM	Private: 60Public: 555	G_{acc} (three fold): 98.33 G_{acc} (ten-fold): 96.67
Xu et al. [20]	Histogram based feature	–	–	Overlap ratio: 73.2 CDR error: 0.091
Matsopoulos [21]	Self-organizing maps	ANN	127	Classification rate: 87.5
Annu and Justin [22]	Wavelet energy features	PNN	–	95%
Dua et al. [11]	Wavelet based energy features	SMO	60	G_{acc}: 93
Mookiah and Faust [12]	Higher order spectra (HOS), trace transform (TT), and discrete wavelet transform (DWT)	SVM	60	G_{acc}: 91.67 G_{sen}: 90 G_{spe}: 93.33
Simonthomas [13]	Haralick texture features	KNN	60	G_{acc}: 98
Gayathri et al. [14]	Wavelet energy features	ANN	–	G_{acc}: 97.6
Gajbhiye et al. [15]	Wavelet and geometric moment features	SVM, KNN, error back-propagation training algorithm (EBPTA)	350	G_{acc}: 86.57
Chrastek et al. [16]	Morphological operations, Hough transform, and an anchored active contour model.	Linear discriminant analysis, classification trees, and bootstrap aggregation	–	G_{acc}: 72.3
Yin et al. [17]	Circular Hough transform and optimal channel selection	Unsupervised	325	CDR error: 0.10
Fink et al. [19]	Independent component analysis	KNN	120	G_{acc}: 91
Acharya et al. [24]	LCP + texton	KNN	702	G_{acc}: 95.7 G_{sen}: 96.2 G_{spe}: 93.7
Maheshwari et al. [32]	VMD and entropy	SVM	488	G_{acc}: 95.19 G_{sen}: 93.62 G_{spe}: 96.71
Raghavendra et al. [45]	Radon + MCT + GIST + LSDA	SVM	1000	G_{acc}: 97.00 G_{sen}: 97.80 G_{spe}: 95.80
Chen et al. [43]	CNN	–	1676	AUC: 0.887
Proposed	*Eighteen* **layer CNN**	**LDA**	**1426**	$\boldsymbol{G_{acc}}$**: 98.13** $\boldsymbol{G_{sen}}$**: 98.00** $\boldsymbol{G_{spe}}$**: 98.30** $\boldsymbol{G_{PPV}}$**: 98.79**

*G_{acc}: accuracy, G_{sen}: sensitivity, G_{spe}: specificity.

Although there have been a significant number of techniques proposed in the literature, it is required to develop an efficient algorithm using maximum number of subjects. Raghavendra et al. [45] have developed a novel expert system using GIST descriptor and SVM classifier. They achieved maximum performance of 97% accuracy for nineteen features using 1000 fundus images. Recently, Chen et al. [43] have used CNN for glaucoma detection by using region of interest (ROI) segmented images to select the optic nerve head from the images. But, our proposed work is fully automated deep learning architecture which can classify even early stage of glaucoma. Generally, convolution neural networks (CNN) extract the localized features from input images and convolution is performed with image patches using filters. Filter responses are pooled repeatedly and refiltered, and the output feature vector of resulting deep feed-forward network architecture are eventually classified [25–27]. The details of the developed model is presented in the subsequent sections.

2. Deep learning framework

Nowadays, image classification is performed using deep learning technique [29–31]. It integrates both feature extraction and classification. These methods can achieve promising results using complex networks built with large scale data. In this work, we have proposed a novel convolutional neural network (CNN) architecture to detect the glaucoma automatically with highest performance. During training our network, the features are extracted from the input images yielding a robust deep CNN model and it efficiently classifies the unknown image during the testing phase. The detailed structure of the proposed method is described in following sections.

2.1. Convolutional neural network (CNN)

The CNN is a deep learning model which consists of various network layers such as image input layer, convolution layer, max pooling, average pooling, rectified linear unit etc. Depending on the size of the input, the number of layers can be increased or decreased. It is not necessary to use all the layers in the network. The deeper the network, the better it learns. It can self-learn and self-organize without any supervision [7,33]. But increasing the depth of the network, increases the computational time, which is not preferred. In this work, we have decided to obtain the maximum output with minimum number of layers by efficiently choosing the network parameters. The advantage of CNN is that, it does not need any pre-processing or handcrafted feature extraction by other methods. In general, features are extracted in a hierarchical manner by mapping raw pixels of the input image and further it is classified using fully connected layers. The network parameters are intelligently tuned to obtain the highest classification performance. The description of different units of CNN is given below:

2.1.1. Image input layer

The image input layer is the first layer and should be present in all networks. It takes the input to the network. In case of images, it can use 2-D as well as 3-D images. Only the dimension of the image should be initialized into this layer [25].

2.1.2. Convolutional layer

This layer performs convolution operation on the input image. A window is moved over the input image with a stride that is specified by the user. After performing convolution, it generates feature maps which are used as input to the next layer [26,27].

2.1.3. Batch normalization layer

This layer potentially helps in both faster learning as well as boosting overall performance. It also allow normalized data samples to flow between intermediate layers which permit us to use higher learning rates and speed up the overall learning process [27].

2.1.4. Rectified linear unit (ReLu)

It is a part of convolutional layer in which for each element of the input the thresholding operation is performed i.e., value less than zero is set to zero. This reduces data redundancy and keeps the important features intact. The size of the output of this layer is same as the previous layer.

2.1.5. Max pooling layer

In this layer, max pooling is applied on each feature map to reduce the size. The value of stride is usually chosen by the user. The maximum value over the window is considered and the window is replaced by that number. The output size of this layer is lesser than that of the previous layer [25–27].

2.1.6. Fully connected layer

The neurons of the previous layer i.e. max pooling layer will be taken and connected to each and every neuron in this layer. The output of this layer will be the number of classes of classification [28].

2.1.7. Soft-max layer

This layer applies a soft-max function to the input data sample. Mathematically, it is a normalized exponential function, which squashes multi-dimensional data samples in the range 0–1. It helps to reduce outliers without removing from the data sample. Further, classification layer holds loss function, output label and size. Fig. 2 presents overview of the proposed CNN architecture.

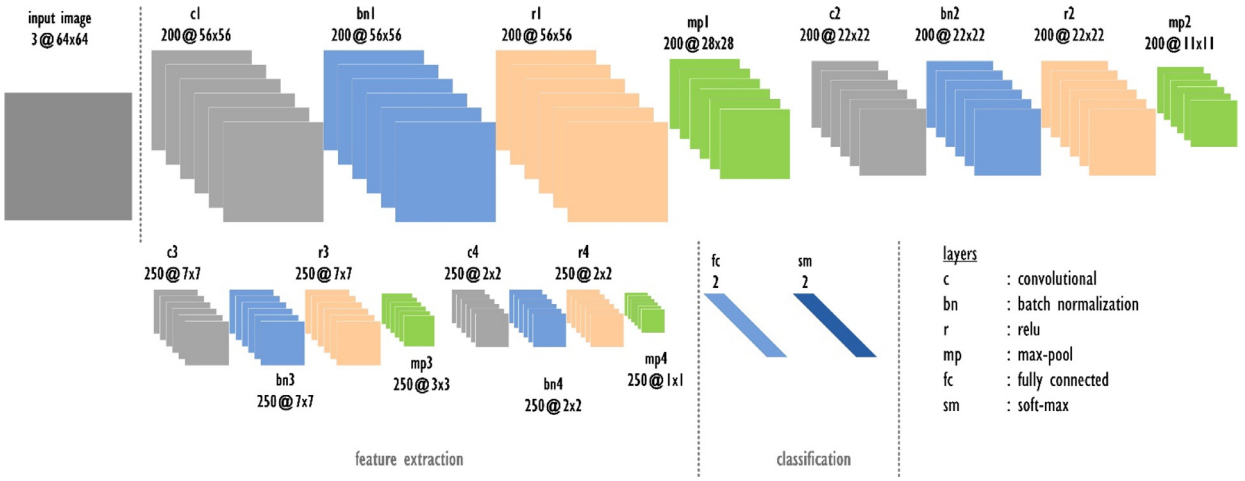

Fig. 2. Overview of the proposed CNN architecture.

Table 2
Description of proposed *eighteen* layer CNN architecture.

Layers	Layer name	Maps and neurons	Kernel
0	Image input	$3@64 \times 64$	–
1	Convolution	$200@56 \times 56$	9×9
2	Batch normalization	Batch normalization	–
3	ReLU	ReLU	–
4	Max-pooling	$200@28 \times 28$	2×2
5	Convolution	$200@22 \times 22$	7×7
6	Batch normalization	Batch normalization	–
7	ReLU	ReLU	–
8	Max-pooling	$200@11 \times 11$	2×2
9	Convolution	$250@7 \times 7$	5×5
10	Batch normalization	Batch normalization	–
11	ReLU	ReLU	–
12	Max-pooling	$250@3 \times 3$,	2×2
13	Convolution	$250@2 \times 2$	2×2
14	Batch normalization	Batch normalization	–
15	ReLU	ReLU	–
16	Max pooling	$250@1 \times 1$	2×2
17	Fully connected	2	–
18	Soft-max	2	–
19	Classification output	Crossentropyex	–

2.2. Methodology

2.2.1. Architecture

CNNs are made up of 2 parts: (i) convolutional layer and max-pool layer, where input of every layer is the output of the preceding layer which act as a feature extractor; (ii) fully connected layer, where the extracted features are classified. Generally, it is a hierarchical feature extractor which maps the input image intensities to a feature vector. The last layer i.e., fully connected layer performs the classification followed by logarithmic soft-max activation function, as they have only one output neuron for every class. All the parameters are tuned for less misclassification error over training set. Overview of our proposed CNN framework is given in Fig. 2. Table 2 shows the descriptions of each layer.

2.2.2. Training and testing

The complete dataset is divided into *two* parts; (i) training and (ii) testing. Initially, 70% randomly selected samples are used for training and remaining 30% are used for testing the developed network. We have used 589 normal images and 837 abnormal images in this work. So, we have used 70% of the images for training (412 normal and 586 glaucoma). This process it repeated for *fifty* times with random training and testing partitions.

The training images are used as input and are used to train the network. The training options used are:

- *Solver name*: Stochastic gradient descent momentum training. It tries to find the direction in which the objective function can be reduced. It also known as steepest descent.

Fig. 3. Sample normal and glaucoma fundus images.

Table 3
Performance of the proposed CNN model for the input size 64×64.

Learning rate	$G_{acc.}$ (%)	$G_{sen.}$ (%)	$G_{spe.}$ (%)	G_{PPV} (%)
0.1	97.42	97.21	97.74	98.38
0.01	97.66	97.60	97.74	98.39
0.001	**98.13**	**98.00**	**98.30**	**98.79**
0.0001	92.28	90.03	95.48	96.58

- *Learning rate:* If the learning rate is too low, training will take a long time. But if it is high, the training may get stuck at a suboptimal result. We have used the training rate 0.1, 0.01, 0.001 and 0.0001 in this work.
- *Epochs:* It is single pass training network followed by validation of the testing set. The maximum epochs used are 20.

3. Experiments

3.1. Image dataset

The retinal fundus images have been obtained from Kasturba Medical College, Manipal, India. There are a total of 589 normal images and 837 glaucoma images. Zeiss FF 450 Fundus camera is used to capture all the images and all acquired images are converted to jpeg format for further processing. Institution ethical approval was taken before acquiring the fundus images. The sample fundus images are shown in Fig. 3.

3.2. Results

In order to perform the systematic evaluation, we have resized all the input fundus images to 64 $\times$ 64 and are subjected to CNN. The complete algorithm is developed in MATLAB and executed using a system configuration of Intel Xeon CPU E3-1225, 3.3 GHz, 16 GB RAM with GPU.

The first part of the evaluation is carried out with images of size 64×64 with a learning rate of 0.1, 0.01, 0.001 and 0.0001. After dividing data set into training and testing set, algorithm is run and different performance parameters such as accuracy, sensitivity, specificity and positive predictive value (PPV) are computed for the evaluation. The highest performance is obtained with a learning rate of 0.001. We obtained 98.13% accuracy, 98% sensitivity, 98.30% specificity and 98.79% PPV as shown in Table 3. In order to generalize our experiment and results, we have repeated (iterations) our experiments *fifty* times and we have calculated the average of all the performance parameters for all iterations. The obtained results are presented in Table 4. Fig. 4 shows the graph of accuracy (%) of the model versus different iterations for different learning rates.

4. Discussion

Generally, maximum number of images need to be used with CNN for better performance [7,33]. In this work, we have used 1426 fundus images to develop the model which consists of *eighteen* layers as shown in Fig. 2 and Table 2. At learning

Table 4
Average performance of the proposed CNN model for *fifty* iterations.

Learning rate	$G_{acc.}$ (%)	$G_{sen.}$ (%)	$G_{spe.}$ (%)	G_{PPV} (%)
0.1	94.14	94.08	94.23	95.89
0.01	95.48	95.68	95.19	96.60
0.001	**95.60**	**95.50**	**95.74**	**96.96**
0.0001	88.67	86.21	92.16	94.02

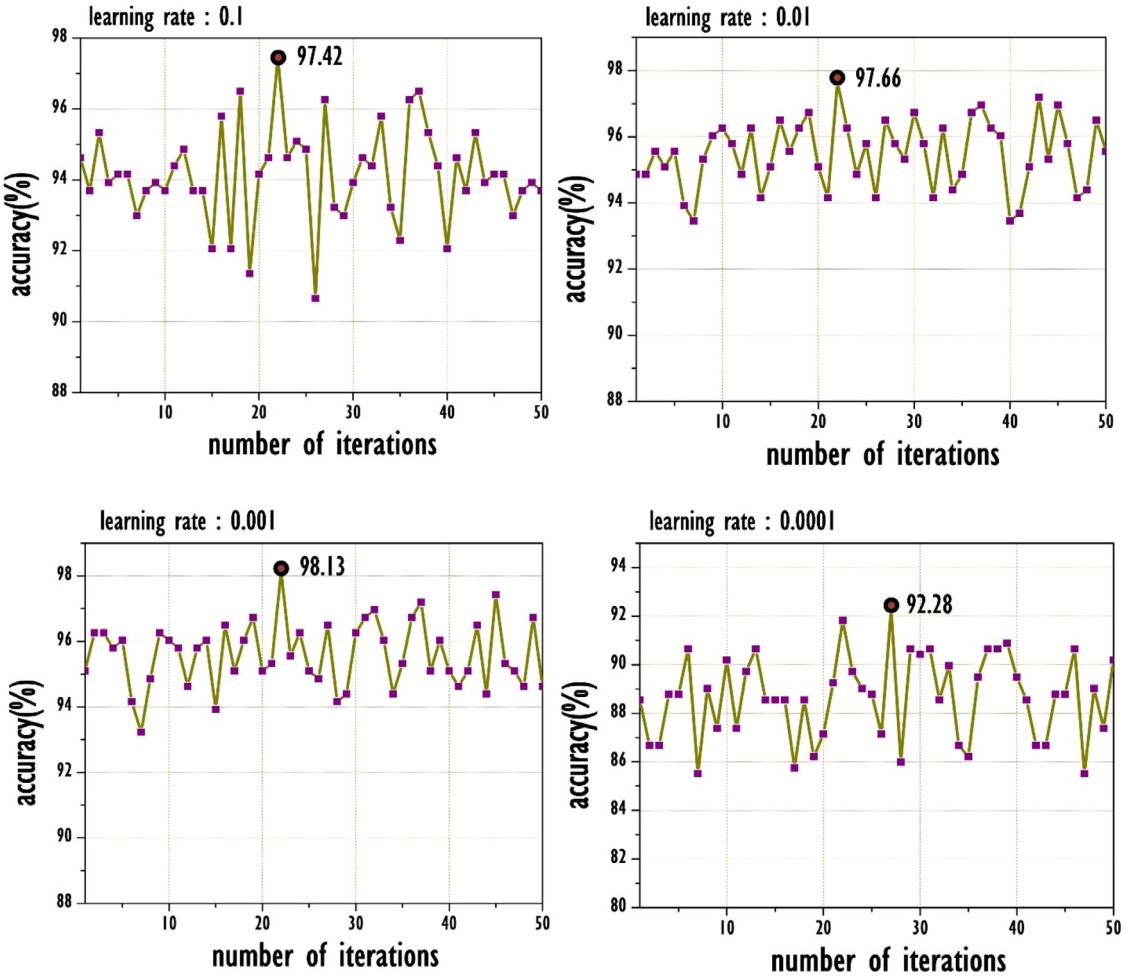

Fig. 4. Plot of accuracy (%) of the model versus different iterations.

rate 0.1, 0.01 and 0.0001, the results are comparatively low. This is because at this particular learning rate, the network may might miss the subtle important information. The model attained the best performance for 0.001 learning rate by gradually capturing minute detailed features from the input images. Another factor that affected the results is the size of the images. The fine detailed information may be lost when small size images are fed to CNN leading to poor performance. But when the number of image input samples are more, taking a smaller sized image as an input is affordable as the network will train with greater number of images. Taking bigger size input samples also increases the computational time. It is observed that image size of 64×64 is suitable size for our model which fetch maximum performance for the developed network. In addition, our model consists of different sized kernels, which captures minute changes and boost the overall performance of the model. The developed algorithm achieved the highest specificity of $\approx$ 99% which confirms that the algorithm detects almost all abnormal cases as abnormal. Hence, clinicians can concentrate more on normal cases. Also we have achieved the best classification performance by feeding the original image without any pre-processing steps. It can be observed that our method is the first attempt in experimenting maximum number of fundus images (1426) and achieved highest performance compared to other methods in the literature (Ref. Table 1). To the best of our knowledge, this is the first fully automated

CNN architecture for the CAD of glaucoma using digital fundus images. Also, our model is robust as it gives consistent performance for all iterations.

There are several advantages of using CNN for the automated detection of glaucoma. One of the main advantages is the elimination of conventional steps such as feature extraction, dimensionality reduction and feature ranking. It automatically extracts the features by generating feature maps after every layer and decides itself the best performing features. This saves lot of time and memory. Another advantage of CNN is that CNN does not require the pre-processing steps which may influence the performance.

To obtain the optimum performance, CNN requires maximum number of images. It is not possible to generalize the system with less number of images. Also, increasing the number of images, increases the number of layers which may boost the computational time of the algorithm. Hence, the parameters of the model need to be judiciously decided to obtain the maximum performance in less time. Also, it may take more time to develop the best performing CNN model. Also, as the number of images increases, it may take more time to converge. So, in order to overcome this problem, we may need to use graphics processing unit (GPU).

Also as a general opinion CNN is more dependent on training images and its performance will decay when testing with negative images which does not belongs to any of the trained classes [44]. In future, we intend to extend this developed CNN model using multi column and multi scale convolutional neural network to detect different stages of glaucoma with huge database by training transformed images rather than raw images.

5. Conclusion

Glaucoma is one of the leading causes of blindness. A large number of populations across the globe is affected by it. The development of CAD tool will assist the ophthalmologists in detecting glaucoma even at mild stage. Our method obtained the highest accuracy, sensitivity, and specificity of 98.13%, 98%, and 98.30%, respectively, for the maximum number of images. The developed CNN model can efficiently detect the class (normal or glaucoma) of unknown image. The main advantage of CNN is, it will take entire image instead of defected part and filtered outputs are pooled together which avoids the sophisticated design of hand-crafted features. Thus, it avoids the segmentations and provides the powerful features to describe normal and glaucoma subjects. The developed toolkit is able to classify almost all glaucoma images correctly. Hence, the ophthalmologists need to focus their attention more on the normal class. This will reduce their workload by nearly 50%. Our developed model can aid the ophthalmologists to cross check their clinical diagnosis. In future, our developed model can be used to detect the glaucoma at an early stage and help in advising early treatment for patients.

References

[1] K. Barton, R.A. Hitchings, Medical management of glaucoma, in: Medical Management of Glaucoma, Springer Healthcare Ltd, 2013, pp. 71–100.
[2] J. Nayak, R. Acharya, P.S. Bhat, N. Shetty, T.-C. Lim, Automated diagnosis of glaucoma using digital fundus images, J. Med. Syst. 33 (5) (2009) 337.
[3] http://www.mayoclinic.org/diseases-conditions/glaucoma/basics/symptoms/con-20024042 (accessed 14 June, 2017).
[4] http://www.glaucoma.org/glaucoma/diagnostic-tests.php (accessed 21 July, 2017).
[5] U. Rajendra Acharya, E.Y.K. Ng, L.W.J. Eugene, K.P. Noronha, L.C. Min, K. Prabhakar Nayak, S.V. Bhandary, Decision support system for the glaucoma using Gabor transformation, Biomed. Signal Process. Control 15 (2015) 18–26.
[6] H. Fujita, Y. Uchiyama, T. Nakagawa, D. Fukuoka, Y. Hatanaka, T. Hara, G.N. Lee, et al., Computer-aided diagnosis: the emerging of three CAD systems induced by Japanese health care needs, Comput. Methods Programs Biomed. 92 (3) (2008) 238–248.
[7] U. Rajendra Acharya, H. Fujita, O. S. Lih, Y. Hagiwara, J. H. Tan, and M. Adam. "Automated detection of arrhythmias using different intervals of tachycardia ECG segments with convolutional neural network." Inf. Sci., 405(2017): 81–90.
[8] K.P. Noronha, U. Rajendra Acharya, K. Prabhakar Nayak, R.J. Martis, S.V. Bhandary, Automated classification of glaucoma stages using higher order cumulant features, Biomed. Signal Process. Control 10 (2014) 174–183.
[9] M.R.K. Mookiah, U.R. Acharya, C.M. Lim, A. Petznick, J.S. Suri, Data mining technique for automated diagnosis of glaucoma using higher order spectra and wavelet energy features, Knowl.-Based Syst. 33 (2012) 73–82.
[10] S. Maheshwari, R.B. Pachori, U.R. Acharya, Automated diagnosis of glaucoma using empirical wavelet transform and correntropy features extracted from fundus images, IEEE J. Biomed. Health Inf. 21 (3) (2016) 803–813.
[11] S. Dua, U. Rajendra Acharya, P. Chowriappa, S. Vinitha Sree, Wavelet-based energy features for glaucomatous image classification, IEEE Trans. Inf. Technol. Biomed. 16 (1) (2012) 80–87.
[12] M.R.K. Mookiah, O. Faust, Automated glaucoma detection using hybrid feature extraction in retinal fundus images, J. Mech. Med. Biol. 13 (01) (2013) 1350011.
[13] S. Simonthomas, N. Thulasi, P. Asharaf, Automated diagnosis of glaucoma using Haralick texture features, in: Proceedings of the 2014 International Conference on Information Communication and Embedded Systems (ICICES), IEEE, 2014, pp. 1–6.
[14] R. Gayathri, P.V. Rao, S. Aruna, Automated glaucoma detection system based on wavelet energy features and ANN, in: Proceedings of the 2014 International Conference on Advances in Computing, Communications and Informatics (ICACCI), IEEE, 2014, pp. 2808–2812.
[15] G.O. Gajbhiye, A.N. Kamthane, Automatic classification of glaucomatous images using wavelet and moment feature, in: Proceedings of the 2015 Annual IEEE India Conference (INDICON), IEEE, 2015, pp. 1–5.
[16] R. Chrástek, M. Wolf, K. Donath, H. Niemann, D. Paulus, T. Hothorn, B. Lausen, R. Lämmer, C.Y. Mardin, G. Michelson, Automated segmentation of the optic nerve head for diagnosis of glaucoma, Med. Image Anal. 9 (4) (2005) 297–314.
[17] F. Yin, J. Liu, D.W.K. Wong, N.M. Tan, C. Cheung, M. Baskaran, T. Aung, T.Y. Wong, Automated segmentation of optic disc and optic cup in fundus images for glaucoma diagnosis, in: Proceedings of the Twenty-Fifth International Symposium on Computer-based Medical Systems (CBMS), IEEE, 2012, pp. 1–6.
[18] V. Grau, J. Crawford Downs, C.F. Burgoyne, Segmentation of trabeculated structures using an anisotropic Markov random field: application to the study of the optic nerve head in glaucoma, IEEE Trans. Med. Imaging 25 (3) (2006) 245–255.
[19] F. Fink, K. Worle, P. Gruber, A.M. Tome, J.M. Gorriz-Saez, C.G. Puntonet, E.W. Lang, ICA analysis of retina images for glaucoma classification, in: Proceedings of the Thirtieth Annual International Conference of the IEEE Engineering in Medicine and Biology Society, EMBS 2008, IEEE, 2008, pp. 4664–4667.
[20] Y. Xu, D. Xu, S. Lin, J. Liu, J. Cheng, C. Cheung, T. Aung, T. Wong, Sliding window and regression based cup detection in digital fundus images for glaucoma diagnosis, Med. Image Comput. Comput.-Assist. Interv. 14 (2011) 1–8.

[21] G.K. Matsopoulos, P.A. Asvestas, K.K. Delibasis, N.A. Mouravliansky, T.G. Zeyen, Detection of glaucomatous change based on vessel shape analysis, Comput. Med. Imaging Graph. 32 (3) (2008) 183–192.
[22] N. Annu, J. Justin, Automated classification of glaucoma images by wavelet energy features, Int. J. Eng. Technol. 5 (2) (2013) 1716–1721.
[23] U.R. Acharya, S. Dua, X. Du, C.K. Chua, Automated diagnosis of glaucoma using texture and higher order spectra features, IEEE Trans. Inf. Technol. Biomed. 15 (3) (2011) 449–455.
[24] U Rajendra Acharya, S. Bat, J.EW Koh, S.V Bhandary, H. Adeli, A novel algorithm to detect glaucoma risk using texton and local configuration pattern features extracted from fundus images, Comput. Biol. Med. 88 (2017) 72–83.
[25] M. Riesenhuber, T Poggio, Hierarchical models of object recognition in cortex, Nat. Neurosci. 2 (1999) 1019–1025.
[26] D. Cireşan, U. Meier, J Masci, A committee of neural networks for traffic sign classification, in: Proceedings of the 2011 International Joint Conference on Neural Networks (IJCNN), IEEE, California, USA, 2011, pp. 1918–1921.
[27] D. Scherer, A. Müller, S Behnke, Evaluation of pooling operations in convolutional architectures for object recognition, in: Proceedings of the 2010 International Conference on Artificial Neural Networks, Springer, 2010, pp. 82–91.
[28] T. Serre, L. Wolf, T Poggio, Object recognition with features inspired by visual cortex, in: Proceedings of the 2005 Computer Vision and Pattern Recognition Conference, 2005, pp. 994–1000.
[29] S. Lawrence, C.L. Giles, Ah Chung Tsoi, A.D. Back, Face recognition: a convolutional neural-network approach, IEEE Trans. Neural Networks 8 (1) (1997) 98–113.
[30] U.R. Acharya, H. Fujita, O.S. Lih, M. Adam, J.H. Tan, C.K. Chua, Automated detection of coronary artery disease using different durations of ECG segments with convolutional neural network, Knowl.-Based Syst. 132 (2017) 62–71 15 September.
[31] J.H. Tan, UR. Acharya, S.V Bhandary, K.C. Chua, S. Sivaprasad, Segmentation of optic disc, fovea and retinal vasculature using a single convolutional neural network, J. Comput. Sci. 20 (2017) 70–79.
[32] S. Maheshwari, R.B. Pachori, V. Kanhangad, S.V. Bhandary, U.R. Acharya, Iterative variational mode decomposition based automated detection of glaucoma using fundus images, Comput. Biol. Med. 88 (2017) 142–149.
[33] UR. Acharya, H. Fujita, S.L. Oh, U Raghavendra, J.H. Tan, M. Adam, A. Gertych, Y. Hagiwara, Automated identification of shockable and non-shockable life-threatening ventricular arrhythmias using convolutional neural network, Fut. Gen. Comput. Syst. 79 (2017) 952–959.
[34] T.C. Lim, S. Chattopadhyay, U.R. Acharya, A survey and comparative study on the instruments for glaucoma detection, Med. Eng. Phys. 34 (2) (2012) 129–139.
[35] UR. Acharya, EYK. Ng, J.S. Suri, Image Modeling of the Human Eye, Image Modeling of the Human Eye, Artech House, 2008.
[36] R.R.A. Bourne, The optic nerve head in glaucoma, Commun. Eye Health 19 (59) (2006) 44–45.
[37] A. Sommer, J.M. Tielsch, J. Katz, H.A. Quigley, J.D. Gottsch, J. Javitt, K. Singh, Relationship between intraocular pressure and primary open angle glaucoma among white and black Americans. The baltimore eye survey, Arch. Ophthalmol. 109 (8) (1991) 1090–1095.
[38] H.A. Quigley, A.T. Broman, The number of people with glaucoma worldwide in 2010 and 2020, Br. J. Ophthalmol. 90 (3) (2006) 262–267.
[39] H. Goldmann, T. Schmidt, Applanation tonometry, Ophthalmologica 134 (1957) 221–242.
[40] C.F. Burgoyne, in: Pearls of Glaucoma Management, Springer, Berlin, Heidelberg, 2010, p. 1. Chapter 1.
[41] Eye Diseases Prevalence Research Group, Prevalence of open-angle glaucoma among adults in the United States, Arch. Ophthalmol. 122 (2004) 532–538.
[42] U.R. Acharya, et al., Automated screening system for retinal health using bi-dimensional empirical mode decomposition and integrated index, Comput. Biol. Med. 75 (2016) 54–62.
[43] X. Chen, Y. Xu, D.W.K. Wong, T.Y. Wong, J. Liu, Glaucoma detection based on deep convolutional neural network, in: Proceedings of the Thirty-Seventh Annual International IEEE Conference on Engineering in Medicine and Biology Society (EMBC), 2015, pp. 715–718.
[44] Hossein H., B. Xiao, M. Jaiswal, R. Poovendran, On the Limitation of Convolutional Neural Networks in Recognizing Negative Images, (2017), arXiv:1703.06857v2.
[45] U. Raghavendra, V.B. Sulatha, A. Gudigar, U.R. Acharya, Novel expert system for glaucoma identification using non-parametric spatial envelope energy spectrum with fundus images, Biocybern. Biomed. Eng. (2017). https://doi.org/10.1016/j.bbe.2017.11.002.